Modeling, analysis and motion control of a Pan Tilt Platform based on linear and nonlinear systems.

IMRAN S. SARWAR, JAVAID IQBAL, AFZAAL M. MALIK
College of Electrical and Mechanical Engineering
National University of Sciences and Technology, Rawalpindi, 46000 Pakistan
imransarwar@ceme.edu.pk

Abstract:- This paper deals with the modeling, analysis and controlled motion control of a two degree of freedom pan tilt platform (PTP) for positioning or aiming a device. The PTP has two revolute joints. The PTP is a device that makes it possible for the camera to point in a desired direction when mounted under a carrier such as an aircraft. The objective of this research work is to derive a linear and nonlinear control system of the PTP to point in a desired direction within allowable specifications. To perform the analysis and simulation, all the parameters involved in the system dynamics were identified. To achieve the motion control a feedback control system with PD controllers was simulated and tested for the position control of pan and tilt mechanism. These PD controllers were derived from linear system model were used in nonlinear control system simulation and tested with real system. The nonlinear control system developed in this paper is nearest to the physical system. The motion controller results matched closely with the simulation results.

Key-Words: - Linear model, Nonlinear model, Analysis, Motion control, Security system.

1 Introduction

The schematic of the PTP has two degrees of freedom as shown in fig. 1. The PTP includes a base, a rotatable pan mechanism and a rotatable tilt structure for supporting and orienting the device in a desired direction. It can continuously revolve about the pan axis and 90 degrees of motion range in the tilt axis.

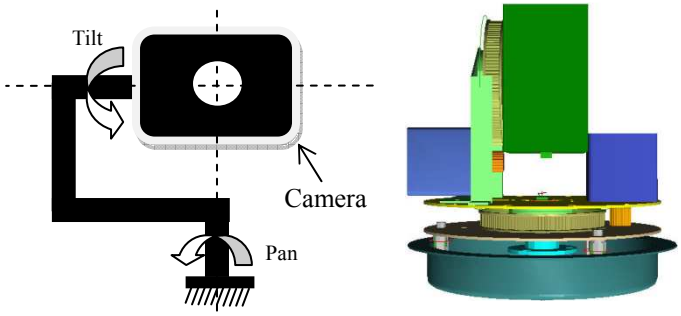

Fig. 1. (a) Schematics and (b) CAD of the PTP

The pan mechanism (base) is rotatable about a pan axis, and the tilt mechanism is rotatable about a tilt axis supported on the base, that is perpendicular to the pan axis. A pan motor and a tilt motor drive the PTP. There is a gear on the shaft of the motor. Through the mechanism of gear, sprocket and belt, the torque is transferred to the structure.

In the world of industrial robotic applications [3] a Proportional-Derivative (PD) controller is often applied; a PD controller doesn't feel the effect of possible changes of load. The ADAMS with Simulink interface is used to obtain the dynamic model and control of closed loop mechanisms [4]. The apparatus in [5] is intended to be used as Control Systems lab trainer to teach the characteristics of PI, PD and PID controls. The [14] has used PTP for detection of moving objects and gesture recognition with an active camera. The method for stability analysis of mechatronics systems with asynchronous machines is discussed in [16]. A graphical technique is introduced for finding all continuous-time and discrete-time proportional integral derivative (PID) controllers that satisfy an H_∞ sensitivity constraint of an arbitrary order transfer function with time delay is presented in [17-18].

We have built two types of models, a linear model and a non-linear model. In the linear model, the Coulomb friction, the centrifugal and the coriolis forces have been neglected. But in the nonlinear model, viscous friction, the Coulomb friction, mass, inertia, centrifugal and coriolis forces have been used. The parameters (friction, mass, inertia, coriolis forces) were identified from experiments or obtained from computer aided design for analysis and simulation purposes. The linear control system along with

proportional-derivative (PD) controllers are analyzed and simulated in Section 3. The nonlinear control system is analyzed and simulated with the PD controllers in Section 4. Both the models have been built according to the following allowable specifications

i. The settling time is expected to be within .1 to .5 seconds.
ii. The steady state error can be tolerated within ± 2%.
iii. The %overshoot is expected to be kept below 22.

The transmissive optoschmitt sensor (OS) consisting of an infrared emitting diode facing an Optoschmitt detector encased in a black thermoplastic housing is used. It checks that %OS does not increase more than the desired value. The encoder attached with motor gives the position of motor shaft. The positioning accuracy of 0.0015rad was achieved for the Pan Tilt Platform. This was achieved by using the DC-motor having encoder of resolution 4096 pulses/revolution. This ensures the steady state error stays below the desired value (<2%). The motion controller for the pan tilt platform is presented in section 5. The results are presented in section 6.

The practicality of this research work can be extended to a broad range of applications. The most apparent use is in security, where there is a strong emphasis on reliably neutralizing threats without risking human life. The unmanned aerial systems (i.e. the PTP on unmanned aerial vehicle) can provide significant reductions in manpower and risk to humans for critical security roles. Such applications include target acquisition, intelligence, surveillance and reconnaissance, border patrol, search and rescue, law enforcement, entertainment and environmental monitoring.

2 Linear System Model

Linear system modeling involves the complex reality with the relatively simple models. The result of nonlinear system is closer to realistic system. But exact equivalence of the model and reality is difficult task. The model should match the real system as closely as possible. The linear model follows from the general nonlinear model under certain assumptions. The nonlinear model based on the Lagrange-Euler equation [2] is as follows.

$$u = M(\theta)\ddot{\theta} + C(\theta,\dot{\theta})\dot{\theta} + F(\dot{\theta}) + g(\alpha)$$

Here $u = \tau$ (torque) is control input and θ is feed-back input vector representing the joint orientation, $M(\theta)$ is a symmetric inertia matrix and $C(\theta,\dot{\theta})$ accounts for centrifugal and coriolis forces. The term $F(\dot{\theta})$ accounts for the viscous friction. The term $g(\alpha)$ accounts for gravity forces, here α is angle between the arm length and force (mg). The term $C(\theta,\dot{\theta})$ is effective when the mass centre begins to move away from the centre of rotation. The effect of centrifugal force becomes evident on the distributed mass of the body. Therefore, centre of PTP is located on the rotational axis of the body and term $C(\theta,\dot{\theta})$ is neglected in linear model. Thus the reduced non-linear system equation for single mechanism (joint) is given as

$$\tau = J_{eff}\ddot{\theta} + f_v\dot{\theta} + f_c sgn(\dot{\theta}) \quad (1)$$

Here, τ = Torque, J_{eff} = Effective inertia, f_v = Viscous friction, f_c =Coulomb friction.

This is a general equation for both the joints and represents the non-linear model of pan and tilt mechanism. The viscous friction is a frictional force that resists objects in motion. The viscous friction is actually a property of the medium in which the motion of the object is occurring. Any fluid medium, such as the grease in the bearings or the air, has an internal resistance to flow, which is represented by the viscous friction. The effective inertial loads of the system are computed from the following relation [1].

$$J_{eff} = \frac{J_a + J_m}{n} + nJ_L \quad (2)$$

J_a = Actuator inertia, J_m = Gear inertia, J_L = Load inertia, n = Gear ratio

Hence, equations (1) and (2) lead to

$$\tau = \left(\frac{J_a + J_m}{n} + nJ_L\right)\ddot{\theta} + f_v\dot{\theta} + f_c sgn(\dot{\theta}) \quad (3)$$

This nonlinear equation still needs to be linearized in order to develop a controller for the system. The nonlinear term in equation (3) is Coulomb friction. It is a frictional force that exists between two objects that are in contact. The close proximity of their surfaces acts to prevent the motion of the objects. This is a very small force with nonlinearity. Therefore, it is neglected in the linear model of the system. Linearization simplifies the pan/tilt model by focusing on each angle (θ_{pan},θ_{tilt}) independently, for the pan and tilt

mechanism. Thus, the linear model takes the following form

$$\tau = J_{eff}\ddot{\theta} + f_v\dot{\theta} \quad (4)$$

This second order differential equation can be expressed in state-space form by introducing the state variables: $x_1 = \theta, x_2 = \dot{\theta}$, with the derivatives as $\dot{x}_1 = \dot{\theta}, \dot{x}_2 = \ddot{\theta}$. Thus the state equations are

$$\begin{aligned} \dot{x}_1 &= x_2 \\ \dot{x}_2 &= -\frac{f_v}{J_{eff}}x_2 + \frac{u}{J_{eff}} \end{aligned} \quad (5)$$

The output equation is

$$y = x_1 \quad (6)$$

Hence the state space model in vector-matrix form is as follows.

$$\begin{aligned} \dot{x} &= \begin{bmatrix} 0 & 1 \\ 0 & -\frac{f_v}{J_{eff}} \end{bmatrix} x + \begin{bmatrix} 0 \\ \frac{1}{J_{eff}} \end{bmatrix} u \\ y &= [1 \quad 0]x \end{aligned} \quad (7)$$

Here

$$x = \begin{bmatrix} x_1 \\ x_2 \end{bmatrix}, \dot{x} = \begin{bmatrix} \dot{x}_1 \\ \dot{x}_2 \end{bmatrix}, u = \tau, A = \begin{bmatrix} 0 & 1 \\ 0 & -\frac{f_v}{J_{eff}} \end{bmatrix},$$
$$B = \begin{bmatrix} 0 \\ \frac{1}{J_{eff}} \end{bmatrix}, C = [1 \quad 0] \quad (8)$$

These state-space equations can be solved if the coefficients f_v and J_{eff} are known. These coefficients are determined as follows.

2.1 Parametric identification

The viscous friction has been determined experimentally. The experimentally determined values of viscous friction are presented in table 1.

Table 1
Viscous friction (Nms/rad)

	Positive	Negative
f_v (pan)	0.0013	0.0023
f_v (tilt)	0.0055	0.0045

The forward and reverse values of the viscous friction were averaged to one value to work with system/state-space models. To find the effective inertial loads in the system, we have used a combination of calculation and measurements. The inertial load of the pan and tilt mechanism were analyzed in the CAD model. We have determined the inertial load on each axis in CAD software by adding all the components with the proper weights/densities. The gear inertia was determined separately in Pro-E and the actuator inertia was determined from the motor datasheet. The effective load on each axis is calculated by using equation (2), and is shown in table 2.

Table 2
Inertial loads for pan and tilt mechanism

	J_L ($Kg\ m^2$)	J_m ($Kg\ m^2$)	J_a ($Kg\ m^2$)	n	J_{eff} ($Kg\ m^2$)
Pan mechanism	0.0750	4×10^{-7}	1.6×10^{-6}	$\frac{120}{21}$	0.4286
Tilt mechanism	0.0055	4×10^{-7}	1.6×10^{-6}	$\frac{120}{21}$	0.0314

2.2 Transfer functions

The transfer function for tilt mechanism is found using (7), (8), tables 1, 2, and $G(s) = C(sI - A)^{-1}B$, and is [9] is given below

$$G(s) = \frac{31.6188}{s^2+0.1581s} \quad (9)$$

The tilt mechanism is marginally stable as one of the system poles lies at the origin.

The transfer function for pan mechanism is determined similarly, and is given below

$$G(s) = \frac{2.3333}{s^2+0.0042s} \quad (10)$$

The pan mechanism is also marginally stable as one of the system poles lies at the origin.

3 Linear System with PD Controller

The linear tilt system and linear pan system were controlled by PD controllers as shown in fig. 3.

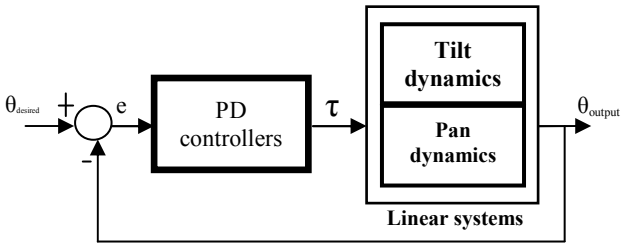

Fig. 3. PTP feedback control system

The tilt system analysis and simulation is shown in section 3.1. Similarly, the pan system analysis and simulation is presented in section 3.3. The compensated tilt system (tilt system and PD controller) analysis and simulation via the root locus method is presented in section 3.2. The compensated pan system (pan system and PD controller) analysis and simulation via the root locus method is presented in section 3.4.

3.1 Tilt system response

The transfer function of tilt system is found in equation (9), section 2.2. According to the root locus technique [9], tilt system has two branches of root locus, symmetrical with respect to the real axis, real-axis segment is [0,-.1581], starting points are the open-loop poles at 0 and -.1581, ending points are the open-loop zeros at ∞ (infinity),∞, real-axis intercept is at -0.079, angle of asymptotes are 90°, 270° and breakaway point is at -0.079. The result of root-locus method, based on simulation performed in Matlab is shown in fig. 5 a. According to the allowable specification; the %OS has to be less than 22%. We have used %OS equal to 5% for which damping ratio (ξ) is equal to 0.6901. The gain (K) has to be designed as shown schematically in fig. 4.

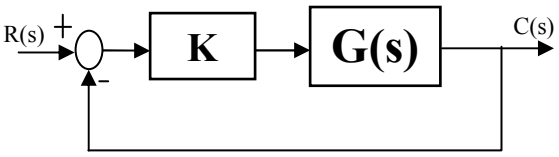

Fig. 4. Closed loop system with gain K

The open-loop transfer function using equation (9) is given as

$$KG(s) = \frac{31.6188K}{s^2 + .1581s} \quad (11)$$

The root locus for the uncompensated system with a damping ratio of 0.69 is represented by a radial line shown in fig. 5(a). We have found dominant pair of poles at -0.0790 ± 0.0830i along the damping ratio line for a gain K = 0.00041494. The uncompensated system step response is shown in fig. 5(b). The closed loop transfer function (T(s)) based on (11) is as follows

$$T(s) = \frac{0.01314}{s^2+0.1581s+0.01314} \quad (12)$$

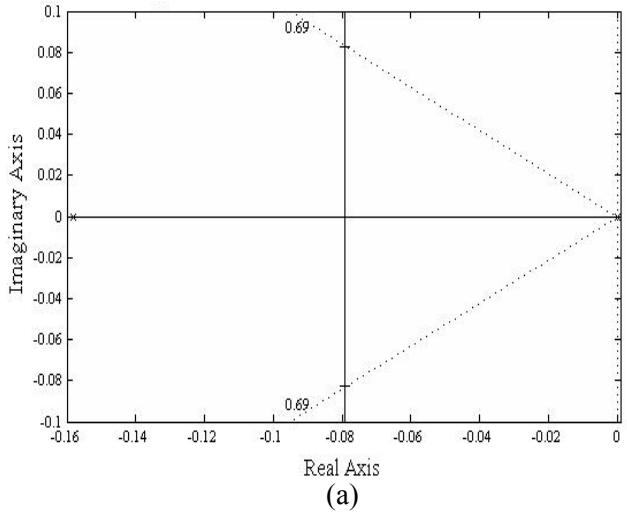

(a)

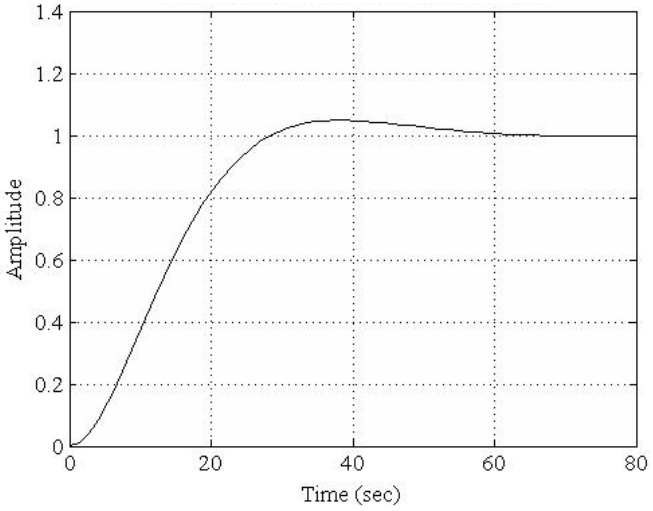

(b)

Fig. 5. Uncompensated system (a) Root locus with radial line (b) step response

As noticed in fig. 5(b), the setting time (50.6 sec) and the steady-state error (12.0342) far exceed the desired performance values. This deficiency has to be compensated by designing the control system.

3.2 Response of tilt system with PD controller

The objective of a PD controller is to drive the T_s to less than 0.5 sec for the unity feedback system. The compensated system is schematically shown in fig. 6.

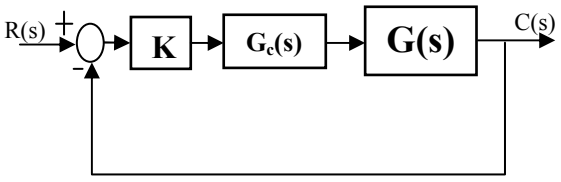

Fig. 6. Closed loop system with compensator

The PD controller is found by using [9]. The PD controller ($G_c(s)$) in Laplace domain is equal to $G_c(s) = s + 21.0808$. The open-loop transfer function resulting for fig. 6 is determined, and is given below

$$KG(s)G_c(s) = K\frac{31.62s+666.6}{s^2+0.1581s} \quad (13)$$

The root locus for the compensated system is shown in fig. 7 (a). A damping ratio of 0.69 is represented by a radial line drawn on the root-locus. We have found dominant pair of poles at -19.3414 ±20.9295i along the damping ratio line for a gain K = 12.184. The compensated system step response is shown in fig. 7 (b). The closed loop transfer function (T(s)) based on (13) is as follows

$$T(s) = \frac{38.21\,s + 805.6}{s^2+38.37\,s + 805.6} \quad (14)$$

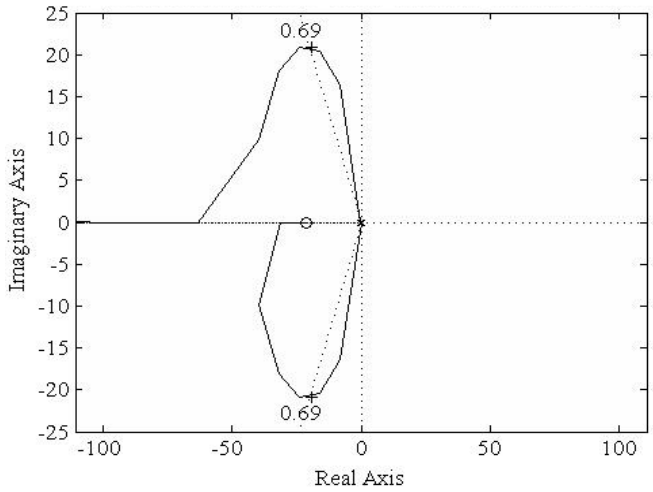

(a)

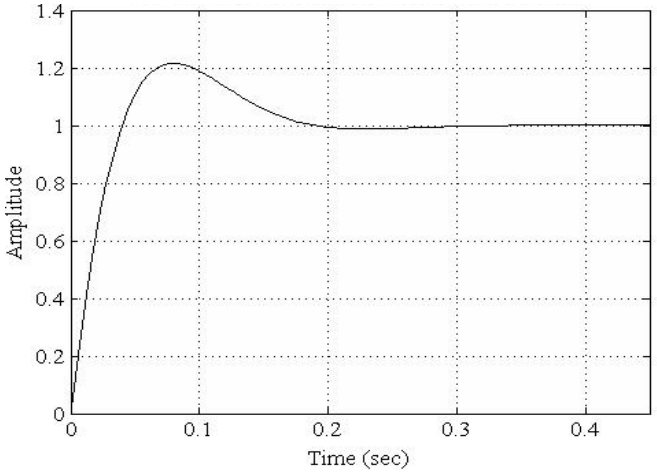

(b)

Fig. 7. Compensated system (a) Root locus with radial line (b) step response

As noticed in fig. 7(b), the setting time (0.2068 sec) and the steady-state error (1.9467×10^{-4}) meet the desired performance values.

3.3 Pan system response

The transfer function of pan system is found in section II; equation (10). According to the root locus technique, pan system has two branches of root locus, symmetrical with respect to the real axis, real-axis segment [0,-.0042] , starting points of open-loop poles at 0, -.0042, ending points of open-loop zeros at ∞ (infinity), ∞, real-axis intercept at -0.0021, angle of asymptotes equal to 90°,270° and breakaway point at -0.0021. The result of root-locus method, based on simulation performed in Matlab is shown in fig. 8 (a). We have used %overshoot equal to 5% for which damping ratio (ξ) is equal to 0.6901. Here gain (K) to be designed via root locus technique is as follows.

$$KG(s) = \frac{2.3333K}{s^2+0.0042s} \quad (15)$$

The root locus for the uncompensated system is shown in fig. 8 (a). A damping ratio of 0.69 is represented by a radial line drawn on the root-locus. We have found dominant pair of poles -0.0021± 0.0022i along the damping ratio line for a gain K = 3.9526e-006. The uncompensated system step response is shown in fig. 8 (b). The closed loop transfer function (T(s)) based on (15) is as follows.

$$T(s) = \frac{9.223*10^{-6}}{s^2+0.0042s+9.223*10^{-6}} \quad (16)$$

As noticed in fig. 8 (b), the setting time (1.9048×10^3 sec) and the steady-state error (455.3986) far exceed the desired performance values. This deficiency has to be compensated by designing the control system.

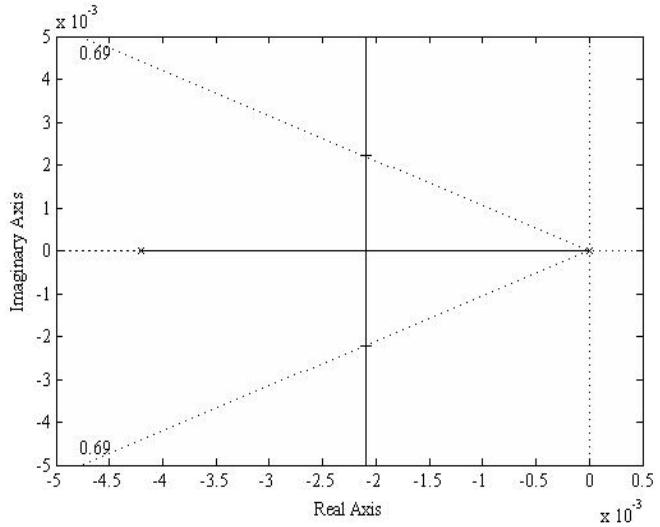

(a)

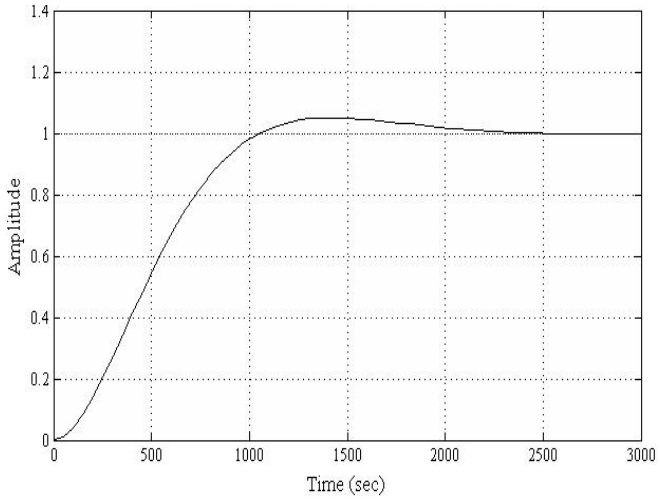

(b)

Fig. 8. Uncompensated system (a) root-locus with radial line (b) step response

3.4 Response of Pan system with PD Controller

The objective of a PD controller is to derive the T_s to less than 0.5 sec for the unity feedback system. The compensated system is shown in fig. 6. The PD controller is found by using [9]. The PD controller ($G_c(s)$) in Laplace domain is equal to $s + 21$.The open-loop transfer function for fig. 6 is given as

$$KG(s)G_c(s) = K\frac{2.333\,s + 49}{s^2+0.0042s} \tag{17}$$

The root locus for the compensated system is shown in fig. 9 (a). A damping ratio of 0.69 is represented by a radial line drawn on the s-plane. We have found dominant pair of poles -20.0502 ±20.9761i along the damping ratio line for a gain K = 17.1843. The compensated system step response is shown in fig. 9 (b). The closed loop transfer function (T(s)) from (17) is given as

$$T(s) = \frac{40.1\,s + 842}{s^2 + 40.1\,s + 842} \tag{18}$$

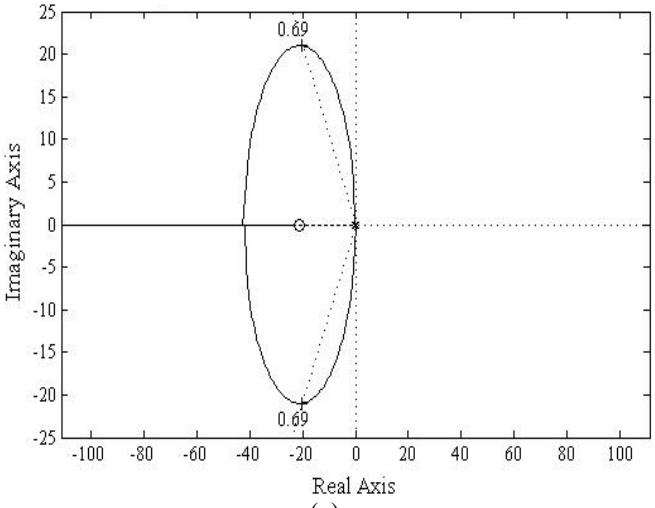

(a)

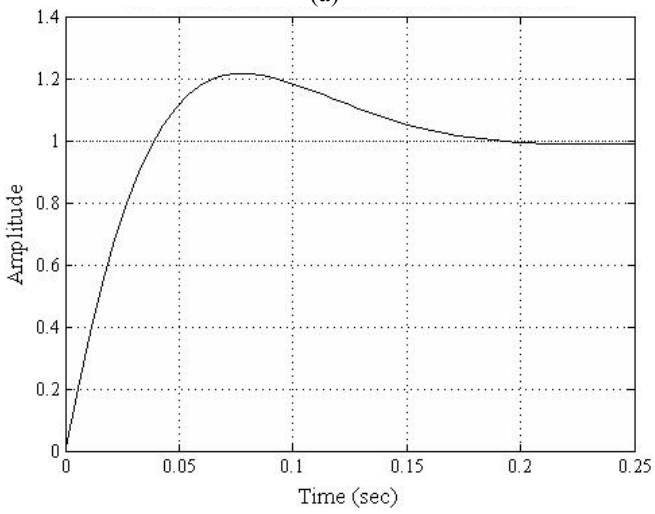

(b)

Fig. 9. Compensated system (a) root-locus with radial line (b) step response

As noticed in fig. 9 (b), the setting time (0.1995 sec) and the steady-state error (1.9467×10^{-4}) meet the desired performance values.

4 Nonlinear control system

The nonlinear model [1] of the PTP including both the Coulomb friction and the gravity effect is given below.

$$\tau = \left(\frac{J_a+J_m}{n} + nJ_L\right)\ddot{\theta} + f_v\dot{\theta} + f_c sgn(\dot{\theta}) + mgl\sin\theta \tag{19}$$

$\theta = Angle\ between\ the\ arm\ length\ and\ force$

Equation (19) is applied separately for both the mechanisms as presented in fig. 10. The required parameters (mass and arm length) were identified from CAD. The Coulomb fraction was identified experimentally to implement the (19). The mass property (physical design) of PTP is summarized in table 3 below:

Table 3
Mass property data

	Surface Area (m^2)	*m* Mass (Kg)	Volume (m^3)	*l* Length (m)
Pan mechanism	0.2008	1.1452	.000224	0.050
Tilt mechanism	0.0858	0.7395	.000402	0.050
PTP	0.2866	1.8847	.000631	-

The Coulomb friction determined accurately can be accounted for and cancelled in the model. The Coulomb friction has been determined experimentally and is given in table 4.

Table 4
Coulomb friction (Nm)

	Positive	Negative
f_c *(tilt)*	0.0500	-0.0550
f_c*(pan)*	0.0400	-0.0405

The values obtained experimentally and available in CAD are presented in table 1, 2, 3 and 4. These values are used in nonlinear model simulation performed in Simulink as explained by Simulink model in fig. 10. The PD controllers were applied as shown in fig. 10. The control law given by [9] is $KG_c = K(K_P e + K_D \dot{e})$. We have used values of *K*, K_D and K_P achieved from section 3. For pan and tilt mechanisms, the controller gains determined in section 3 are given in table 5.

Table 5
Controller Gains

Gains	Pan Mechanism	Tilt Mechanism
K	17.1843	12.184
K_D	1	1
K_P	21.00	21.08

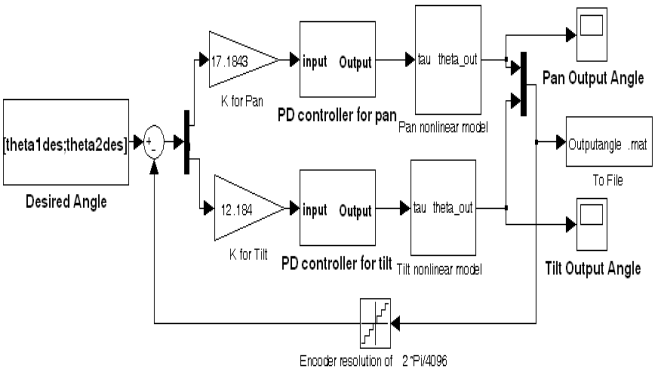

Fig. 10. Pan Tilt Platform Simulation

The PD controllers work with the same gains as found in section 3 for the PTP in the presence of nonlinearities. The results in fig. 11 verified the results obtained in the section 3.

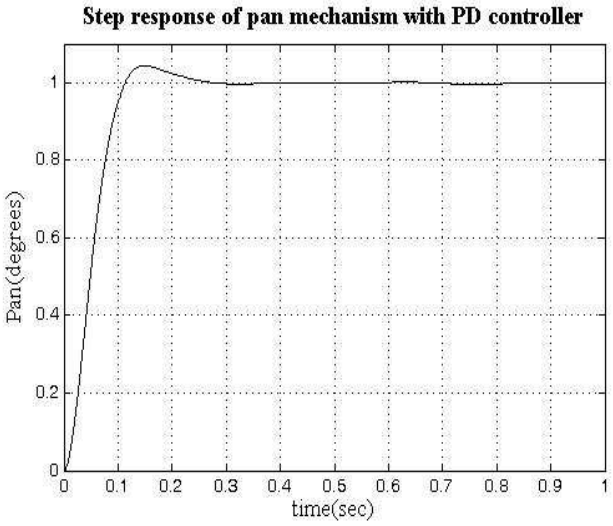

(a)

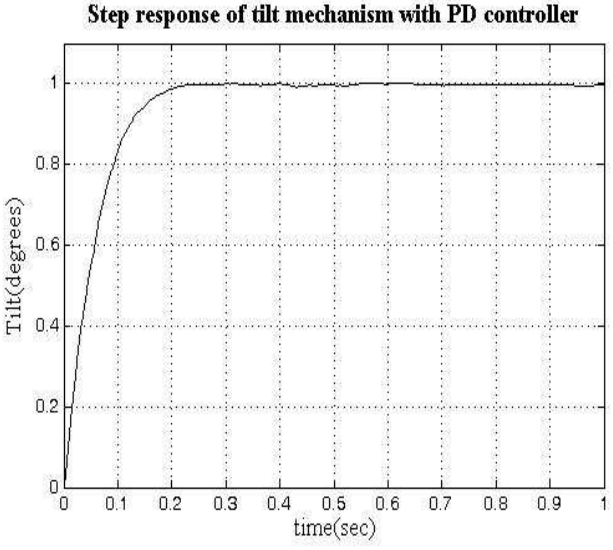

(b)

Fig. 11. Output of (a) Pan (b) Tilt Platform

5 Implementation

The design of a tilt mechanism is intended to perform a tracking task. The input is described in terms of desired angular position of the camera. It is a typical case of an inverse kinematics in the sense that given a predefined objective (output), the input (reference) was determined by using image processing unit (image processing software on a computing unit). We have found in section III and IV the error signal and consequently amplified error signal to the motor of the tilt mechanism. In fig. 12, the input angles come from image processing unit and it takes output of digital camera as input. The 8051 microcontroller has been used as interface between main computer on UAV and LM628 on the control circuit. The assembly code was developed and hex file was written in the flash memory of 80C51.

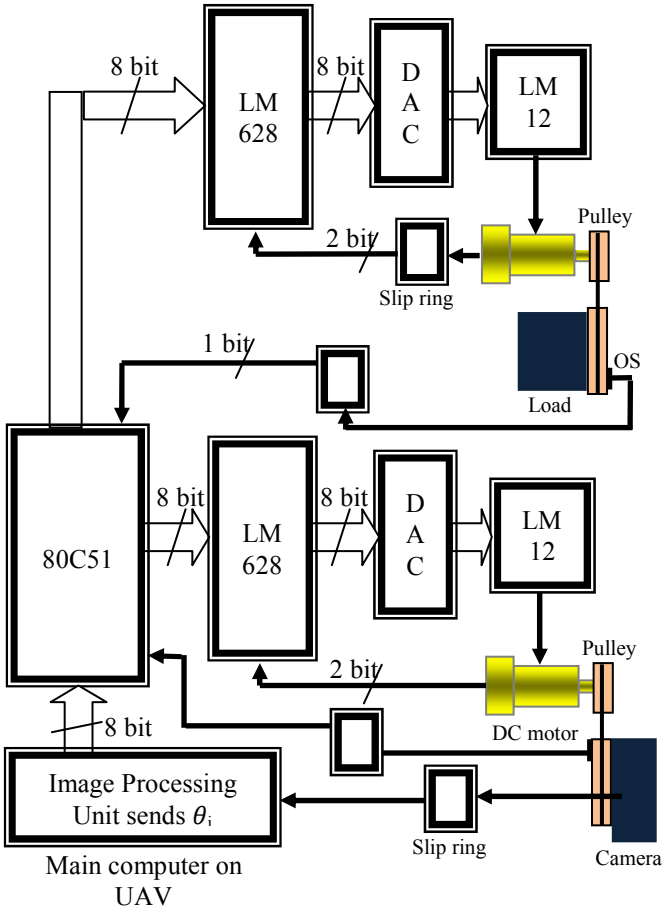

Fig. 12. Schematic of the control card for Pan Tilt Platform

In fig. 13, digital to analog converter (DAC) receives 8 bit signal from LM628 and sends it to the LM12 (power amplifier). Most significant bit of the DAC is the sign bit. When this bit is 1 the output is positive otherwise it is negative.

The LM628 is used due to its capabilities: 32-bit position, velocity, and acceleration registers, programmable digital PID filter with 16-bit coefficients, programmable derivative sampling interval, 8 or 12-bit DAC output data, internal trapezoidal velocity profile generator, velocity, target position, and filter parameters may be changed during motion, position and velocity modes of operation, real-time programmable host interrupts, 8-bit parallel asynchronous host interface and quadrature incremental encoder interface with index pulse input. The controller gain presented in table 5 are feed in the LM628 using 80C51. The LM12 is a power op amp capable of driving ±25V at ±10A while operating from ±30V supplies. The monolithic IC can deliver 80W of sine wave power into a 4W load with 0.01% distortion. A peak dissipation capability of 800W allows it to handle reactive loads such as transducers, actuators or small motors without derating. For stable operation output, capacitors must be greater than 27μF -100μF.

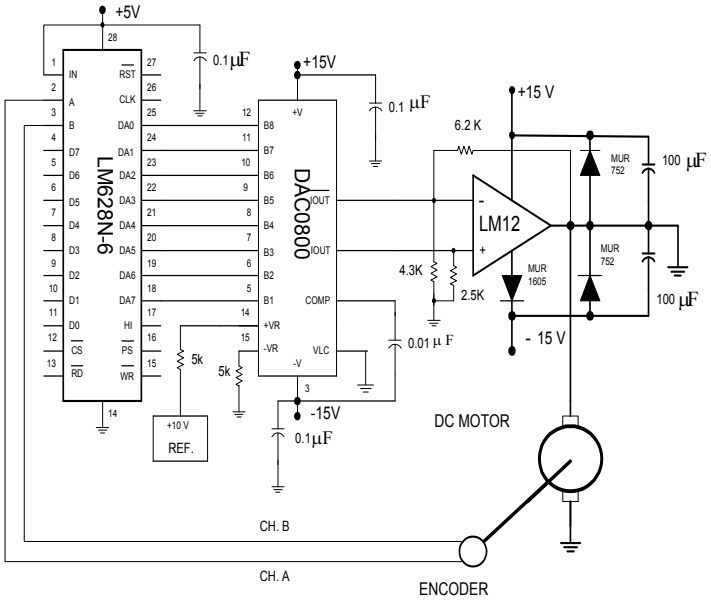

Fig. 13 Drive circuit for DC motor

The algorithm for position control of a pan tilt platform is presented in fig. 14.

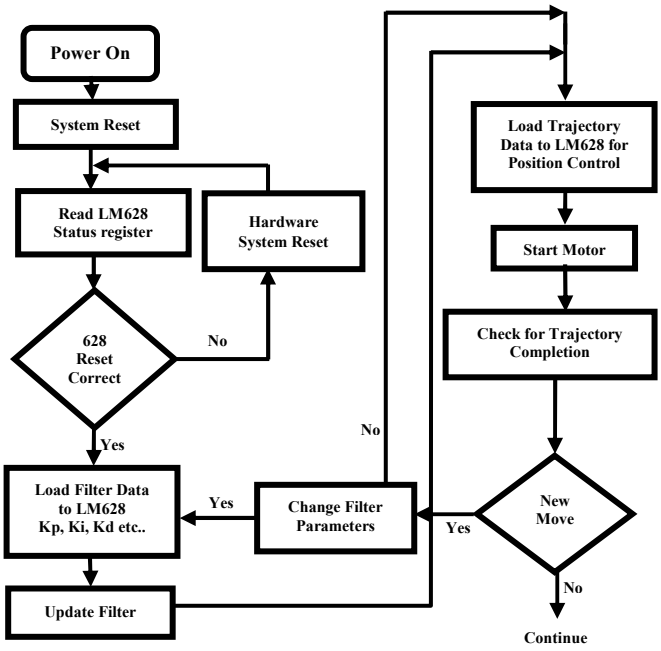

Fig. 14. Load trajectory parameters

The OS are used for initialization of the pan tilt platform at the start and in case of tilt mechanism it also provides the safety and limit for camera movement. The encoders of 4096 pulses/rev are used with motors as shown in fig. 12.

The motion limit of pan mechanism is 0° to 360°. The pan mechanism has ability to rotate continuously, due to slip ring, without damaging the circuit and wires.

After completing the move, the control system will attempt to hold the shaft at its current absolute position. The shaft will feel lightly "spring loaded". If forced away from its desired resting position and released, the shaft will move back to the desired position.

6 Results

Linear and nonlinear modeling of the PTP and its simulation based on feedback control system using the PD controllers for both the models leads to the following conclusions.

- The comparison of linear and nonlinear simulation with PD controllers is shown in table 6. The value of T_s achieved was 0.2 seconds, which is less than the design constraint of 0.5 seconds. Our design leads to a steady-state error of 10^{-3}, which is much less than design constraint of ±2%. Thus our design leads to very reliable results.

Table 6
System models with PD controller

	Linear model		Nonlinear model	
	T_S (seconds)	e_{SS}	T_S (seconds)	e_{SS}
Tilt Mechanism	0.2068	1.9467×10^{-4}	0.20	4.4367×10^{-3}
Pan Mechanism	0.1995	4.9881×10^{-6}	0.21	7.9351×10^{-3}

- It is possible to get the desired performance from the controlled system by choosing the appropriate values of parameters of PD controllers in an involved way based on a trail and error method. However, we have obtained a better solution by a more effective and reliable technique based on modeling and analysis.
- The linear and non-linear model of system with PD controllers gives us desired orientation of camera with a slight difference in the settling time (10^{-2}) and steady-state error (10^{-3}). This is due to the effect of the Coulomb fraction and gravity.
- The implementation results matched closely with the simulation results.

Acknowledgement:

The authors are indebted to the National University of Sciences and Technology, Rawalpindi, Pakistan and the Higher Education Commission of Pakistan for having made this research work possible.

References:

[1] R.J. Schilling, "Fundamental of robotics analysis and control", Prentice Hall, 1990.

[2] H.K. Khalil, "Nonlinear system", Prentice Hall, 3rd edition, 2002, pp. 24.

[3] F.M. Raimondi, T. Raimondi, M.Melluso, "Stochastic Estimate PCA Algorithm for Planar Industrial Manipulator Control", Proceeding of the UKAC-IEE Control 2004 Conference, Bath (U.K.), 2004.

[4] Z. Affi, L. Romdhane, "ADAMS/SIMULINK interface for dynamic modelling and control of closed loop mechanisms", Proceedings of the 7th WSEAS International Conference on automatic control, modeling and simulation, Prague, Czech Republic, 2005, pp. 353-356.

[5] K. Altaf, A. Akhtar, S.U. Rehman, Javaid Iqbal, "Design, implementation and real-time digital control of a cart-mounted inverted pendulum using Atmel AVR Microcontroller", Proceedings of the 6th WSEAS International Conference on Signal

Processing, Robotics and Automation, Corfu Island, Greece, February 16-19, 2007, pp 54-59.

[6] S. Bennett, "The past of PID controllers", Elsevier Science Ltd, Annual reviews in control 25, pp. 43-53, 2001.

[7] B. Rice; Cooper D., "Design and tuning of PID controllers for Integrating (non-self regulating) processes", Proc. ISA 2002 annual meeting, Chicago, 2002, pp. 424-437.

[8] F. Behi, "Kinematic analysis for a six-degree-of-freedom 3-PRPS parallel mechanism", IEEE Journal of Robotics and Automation, Vol. 4, Oct 1988.

[9] N.S. Nise, "Control systems engineering", Wiley student edition, Forth edition, 2004, pp. 515-524.

[10] N. Khongkoom; A. Kanchanathep; S. Nopnakeepong; S. Tanuthong; S. Tunyasrirut; R. Kagawa, "Control of the position DC servo motor by fuzzy logic", Proc. TENCON 2000, vol. 3, 24-27 Sept. 2000, pp. 354 – 357.

[11] I. S. Sarwar, "Design, modeling and control of Pan Tilt Platform for unmanned aerial vehicle", M.S. thesis, Dept. Mechatronics Eng., National University of Sciences and Technology, Rawalpindi, Pakistan, 2006.

[12] J. Zhang; Xu S.; J. Li,"A new design approach of PD controllers", Elsevier, Mar 2005, pp. 329–336.

[13] I. S. Mackenzie, "The 8051 Microcontroller", 4th ed. Prentice-Hall Englewood Cliffs, New Jersey, USA, 1995, pp. 17-115.

[14] K.K. Kim, H.J. Kim, J.Y. Lee, "Motion Analysis for Human-Robot Interaction", 7th WSEAS Int. Conf. on Mathematical methods and computational techniques in electrical engineering, Sofia, Oct 2005, pp. 255-258.

[15] V. Potkonjak, N. Jaksic, "Contribution to a computer-aided choice of D.C. motors for manipulation robots", Robotica, vol. 4, pp. 37-41, 1986.

[16] S. Enache, A. Campeanu, I. Vlad, M.A. Enache, "Original method for stability analysis of mechatronic systems with asynchronous machines", WSEAS transactions on systems and control, Issue 1, Vol. 3, Jan 2008.

[17] T. Emami, J.M. Watkins, "A unified approach for sensitivity design of PID controllers in the frequency domain", WSEAS transactions on systems and control, Issue 5, Vol. 4, May 2009.

[18] T. Emami, J. M. Watkins, "Robust performance characterization of PID controllers in the frequency domain", WSEAS transactions on systems and control, Issue 5, Vol. 4, May 2009.